Link to original published version: *http://dx.doi.org/10.1111/1556-4029.12689*

Citation: Villa, C., Buckberry, J., Cattaneo, C., Frohlich, B. and Lynnerup, N. (2015) Quantitative analysis of the morphological changes of the pubic symphyseal face and the auricular surface and implications for age at death estimation. Journal of Forensic Sciences, 60 (3): 556–565.

Villa C., Buckberry J., Cattaneo C., Frohilich B., Lynnerup N. 2015. *Quantitative analysis of the morphological changes of the pubic symphyseal face and the auricular surface and implications for age at death estimation*. Journal of Forensic Sciences-. Journal of Forensic Sciences, Vol. 60, No. 3, 2015, p. 556–565.

Quantitative analysis of the morphological changes of the pubic symphyseal face and the auricular surface and implications for age at death estimation.

Chiara Villa[1] M.Sc., Jo Buckberry[2] Ph.D., Cristina Cattaneo,[3] M.D., Ph.D., Bruno Frohlich,[4] Ph.D. and Niels Lynnerup,[1] M.D., Ph.D., D.M.Sc.

[1]Laboratory of Biological Anthropology, Department of Forensic Medicine, University of Copenhagen, Denmark;

[2]Biological Anthropology Research Centre, Archaeological Sciences, University of Bradford, UK;

[3]LABANOF, Forensic Anthropology and Odontology Laboratory, Department of Human Morphology, University of Milan, Italy.

[4]Department of Anthropology, Smithsonian Institution, USA

***Corresponding author:**

Chiara Villa

Laboratory of Biological Anthropology,
Department of Forensic Medicine,
University of Copenhagen,
Frederik V's Vej 11, DK-2100 Copenhagen, Denmark.
Email: chiara.villa@sund.ku.dk

Villa C., Buckberry J., Cattaneo C., Frohilich B., Lynnerup N. 2015. *Quantitative analysis of the morphological changes of the pubic symphyseal face and the auricular surface and implications for age at death estimation*. Journal of Forensic Sciences-. Journal of Forensic Sciences, Vol. 60, No. 3, 2015, p. 556–565.

Keywords: forensic science, forensic anthropology, curvature, CT scans, surface scans, 3D models.

ABSTRACT

Age estimation methods are often based on the age-related morphological changes of the auricular surface and the pubic bone. In this study a mathematical approach to quantify these changes has been tested analyzing the curvature variation on 3D models from CT and laser scans. The sample consisted of the 24 Suchey-Brooks (SB) pubic bone casts, 19 auricular surfaces from the Buckberry and Chamberlain (BC) "recording kit" and 98 pelvic bones from the Terry Collection (Smithsonian Institution). Strong and moderate correlations between phases and curvature were found in SB casts (ρ 0.60-0.93) and BC "recording kit" (ρ 0.47-0.75), moderate and weak correlations in the Terry Collection bones (pubic bones: ρ 0.29-0.51, auricular surfaces: ρ 0.33-0.50) but associated with large individual variability and overlap of curvature values between adjacent decades. The new procedure, requiring no expert judgment from the operator, achieved similar correlations that can be found in the classical methods.

One of the most challenging tasks in building a biological profile is the estimation of age-at-death. Several methods were developed during the last century based on the changes in different skeletal regions and new ones are still developing, adapting classical methods to new technologies.

The pelvic bones, in particular the auricular surface and the pubic symphyseal face, have received extensive attention in the literature. Early in the last century, Todd (1) analyzed in detail the morphology of the pubic symphyseal face and described ten ideal phases of development. Most of the subsequent methods represent refinements or adjustments of Todd's work (2-4). The Suchey-Brooks method may be considered the most used in forensic and bio-archaeological contexts (5). It relies on the use of reference casts (6) that illustrate typical stages of bone changes throughout different age intervals both for males and females. The morphological changes of the auricular surface were first investigated by Sashin (7), but the first practical method for estimating the age-at-death was created by Lovejoy and colleagues (8), who described eight stages using different morphological features such as porosity, surface texture and transverse organization. Bedford and colleagues (9) tested and assembled a set of photographs of auricular surfaces that can be used in the application of the method. More recently, Buckberry and Chamberlain (10) separately scored some of the osteological features on which Lovejoy et al.'s method was based, resulting in a more practical method (11, 12). However, the results of the research carried out by Garvin and Passalacqua (5) indicated that the method of Lovejoy et al. (8) is still the most used method.

Both the pubic symphyseal face and the auricular surface are subjected to morphological and degenerative changes with increasing age and all methods analyze and score these changes in a qualitative way. Using 3D reconstruction, obtained with CT or surface scanning, a different approach may be applied: a mathematical and quantitative approach, more objective and not reliant on the experience of the observer, e.g. a curvature analysis. With such approach, we would expect to find largely positive and negative curvature values (reflecting strongly convex and concave surface, respectively) in young adults where the surface is dominated by horizontal ridges and well-marked grooves, in the pubic bone, or by marked transverse organization, in the auricular surface. With increasing age, the curvature values should be lower and more homogenous, since the surface becomes progressively smoother and flatter. Finally, since the surface of the old adults is irregular with increasing porosity and depression, the curvatures should be less homogenous and primarily showing negative values. Only one paper has reported a similar approach for the pubic bone (13); however no test was performed on the auricular surface.

The research objective of this study was to quantify the morphological features of the pelvic bone surfaces (auricular surface and pubic symphyseal face), utilizing the 3D digital nature of CT and laser scanning in order to calculate the curvature of the surface. We first quantified the geometrical changes of the diagnostic features (i.e. ridges and furrows, transverse organization, porosities) on 3D data of Suchey-Brooks pubic bone casts and of the “auricular surface recording kit” on which the method of Buckberry and Chamberlain (10) was developed. Then we applied the same algorithm to a larger sample from the Terry Collection (Smithsonian Institution, Washington D.C., USA).

Materials and Methods

Materials

First analyses were performed on 24 Suchey-Brooks (SB) pubic bone casts (12 females, 12 males), which represented the early and advanced patterns of the six phases of the method (3), and on 19 auricular surfaces composing the "recording kit" assembled by Buckberry and Chamberlain (BC) as representative of the different scores of the features described in their paper (10). Three dimensional files (as STL format- Standard Triangulation Language) were created from CT scans and laser scanner acquisitions. Computed Tomography images were generated using a Siemens Somatom Sensation 4 Multislice spiral scanner with the following parameters: 120kV, 110 mAs, 0.75 mm slice thickness, 0.3 mm slice increment interval. The resulting voxel size was 0.46 x 0.46 x 0.3mm. Surface scans were performed using a 650nm red line laser (optical output power 5mW) and a high resolution camera (CCD monochrome camera with 1024 x 768 resolution, sensitivity of 0.5 lx at 1/15s, gain 20 dB, 30 frame rate with focal length of the lens of 6 mm), with a resolution of 9 x 9 points for mm^2.

The curvature algorithm was then applied on a larger sample. We selected 98 right innominate bones randomly stratified for decades (sex and age distributions shown in Fig. 1) from the Terry Collection (Washington D.C., USA). Only subjects of Caucasian ancestry were included in this study. Initially, 100 bones with no apparent sign of trauma or disease and with intact auricular surface and pubic symphyseal face were selected, but two specimens were later excluded due to pathological conditions detected after performing CT scanning. The bones were scanned with Siemens Somatom Emotion 6 (Smithsonian Institution) at 130kV and 90mAs with 0.63mm slice thicknesses and 0.2mm slice increment resulting in a voxel size of 0.36 x 0.36 x 0.2 mm. Surface scans were acquired with the same instrument and settings described above.

Region of interest (ROI)

In the pubic bone two regions of interest (ROIs) were initially identified: the anterior portion, (Fig. 2a) and the central portion of the pubic symphyseal phase inside the margin (Fig. 2b). The limit of the anterior portion was defined at about 1 centimeter from the pubic symphyseal face vertically oriented. For the auricular surface we considered the internal portion, i.e. the area delimitated by the contour of the joint (Fig. 2c). The 3D data from CT and laser scans were registered and delimitated together to keep consistent ROIs between modalities.

Curvature analysis

Curvature can be defined as the variation of a geometrical object (i.e. a curve or a surface) from being flat. Mathematically, the curvature (K) in two-dimensional space can be defined as the reciprocal of radius (R) of an osculating circle ($K = 1/R$), where the osculating circle is the circle that most closely approximates the curve at a given point. In three dimensions, the curvature depends on the principal curvatures of two orthogonal planes. These describe the maximum curvature (K_{max}) and the minimum curvature (K_{min}) and these two curvatures can be combined in several ways. The *extrinsic curvature* or *mean curvature* (K_m) is used in this study and is defined as the average of the two curvatures, espressed as $K_m = (K_{max}+K_{min})/2$. Conventionally, convex surfaces will yield positive values and concave surfaces negative values, respectively (see (14), for further mathematical explanation)

In this study we calculated curvature using Peyre's Toolbox Graph MATLAB software (15), adapting some of the scripts (16).

We calculated the five variables for each ROI:

- the arithmetic mean of the absolute values of curvature (mean);

- the highest ten percent of the curvature values (highest);
- the lowest ten percent of the the curvature values (lowest);
- the percent of convex surface, i.e curvature values higher than zero (convex);
- and the percent of the flat surface, i.e. the curvature values between -0.01 and 0.01 (flat).

Statistical analysis

The statistical analyses were performed using SPSS software version 20. The linear association between the variables was investigated by calculating the Spearman's rank correlation coefficient (ρ). We calculated the Spearman's correlation between phases and curvature values for the pubic bones casts. For BC "recording kit", correlations were calculated for each features of the Buckberry and Chamberlain method (transverse organization, surface texture, macroporosity, microporosity), excluding the apical change (AC) because this area fell outside the ROI. A total score without this feature (Partial Total Score) was calculated and used in the correlation analysis. For the Terry Collection sample Spearman correlation was calculated to measure the relationship between curvatures values and phases/Partial Total score or decades. Different levels of significance were reported, indicated in the table with different number of stars: 0.05 (*), 0.01 (**) and 0.001 (***). Finally, scatter plots were used to visualize the results of the curvature analysis.

Results

Pubic bone

SB Casts

The visual results of the curvature for the 12 female casts are shown in color coded images (Fig. 3): red and blues colors represent the extreme values of curvature, the highest and the lowest values, respectively; the green highlights the medium values, represented by the flat surface. The first phases are dominated by high ridges in red and furrows in blue. As phase increases, the surface becomes flatter and is dominated by light blue and green colors.

The strength and the significance of the relationship between the curvature and the pubic bone are reported in Table 1. We performed the analysis for both ROIs (anterior and central portions), but the anterior portion was excluded from the subsequent analysis, since it showed weak or moderate correlations with increasing phases in almost all variables and it did not show statistically significant differences. Considering the central portion, the strongest correlation with the increasing phases was found in females, using 3D models from CT-scans. Scatter plots of the arithmetic mean of the absolute values of curvature (mean) and of the percent of flat surface in the two modalities (CT and Laser) are shown in Fig. 4. The two modalities show similar trends, but with a lower dispersion of the points in 3D laser models.

Terry Collection

Correlations obtained using the Terry collection bones are reported in Table 2. Weaker correlations were found than for the pubic bone casts. Only a few cases resulted in a statistically significant correlation; furthermore, the variables that performed better were different between sexes and modalities. For instance, "mean" was significantly correlated with age in females (ρ =0. 29 for both modalities), but not in males. In contrast, "convex" was correlated with the decades only in males (ρ = 0. 51 for laser). These two examples are shown in the scatter plots in Fig. 5. Stronger correlation in both sexes were found applying the SB method directly on the bones: females ρ = 0.63, males ρ = 0.64. These moderate correlations were also statistically significant (p<0.001).

Auricular surface

BC "Recording kit"

The correlation and the levels of significance for the curvature are reported in Table 3, both for the single features of the Buckberry and Chamberlain method (transverse organization; surface texture, macroporosity, microporosity) and the Partial Total Score. Fig. 6 shows the distribution of the mean curvature values and the percent of flat surface versus the Partial Total Score for both modalities.

Terry Collection

The correlations between the curvatures and the Partial Total Score, and between the curvature and the decades are shown in Table 4. Stronger correlations were found in comparison with the pubic bone, excluding the percent of convex surface; this variable did not express the curvature variation of the auricular surface. The correlation values resulting from the curvature analysis are similar to those found between the results of the application of the BC method directly on the bones: total score ρ=0.46, Partial Total Score ρ=0.45 and stage ρ=0.44. All values were significant at p=0.01.The distribution of the curvature values versus the Partial Total Score and the decades for the lowest ten percent of curvature values and for the percent of flat surface are shown in Fig. 7. The results of the Terry Collection are compared with those of the "recording kit" (black filled points): the two groups present similar values. The large dispersion of the data is clearly seen in the scatter plots of the variables versus the decades; decades 70-79 and 80-89 shown major scattering in curvature. Table 5 reported the descriptive statistics of all variables (excluding the % convex) versus the decades for both modalities; the large dispersion and the overlapping among the each decade are clearly visible.

Discussion and Conclusion

The existing methods for age estimation analyze the morphological changes of the pubic bone and the auricular surface only in a qualitative way. We tested a new mathematical approach to quantify the osteological changes of these surfaces by calculating the curvature variation.

We first analyzed the Suchey-Brooks pubic bone casts. Since the original method is based on the evaluation of the changes of the pubic symphyseal face as well as of the borders (ventral rampart, dorsal plateau), we delimited a ROI including both areas. Unexpectedly, we did not observe statistically significant correlation between the curvatures and the age as represented by the phases; we limited the subsequent analysis to the central portion. Here, we found very strong correlation (Table 1): phases I and II are dominated by ridges and furrows corresponding at high absolute values of curvature (Fig. 3), both positive (convex) and negative (concave); with increasing age, these features become smoother and the surface becomes gradually flatter. In addition, we noticed that the curvature analysis highlighted differences between sexes: females showed stronger correlation with less variation than males.

The following step was the application of the same curvature algorithm to the pubic bones of known-age from the Terry Collection. We found a very large dispersion in curvature (Fig. 5), with weaker correlation than those for the SB casts. This is in agreement with the results of Biwasaka and colleagues (17) who applied curvature analysis on a contemporary Japanese sample. We arrived at the same conclusion: it is not possible to discern between phases III- VI from the surface curvature. Biwasaka et al. (17) hypothesized that the exclusion of the ventral rampart could explain the constant curvature after phase IV in their results. We also considered the margins using the anterior area, but we found weak correlations and no statistically significant (Table 1). A possible reason could be that the changes of the central portion and those of the margins occur at different scales and could be not analyzed simultaneously in the 3D models. Separate analysis would need to be carried out to evaluate first the general variation of the surface (ridges and furrows versus a flat surface) and then the local variation of the margins (partial versus complete rim).

For the auricular surface, we performed the first analysis on the original “recording kit” assembled by Buckberry and Chamberlain, since only photographs (9) accompany the system of Lovejoy's et al.(8). We decided to delimit the ROI of the auricular surface at the internal part of the joint for two reasons: the first one because the border of the joint was easy to follow and allowed a precise and repeatable delimitation; the second one because the apical change had the lowest correlation with age in the original method (10). We calculated the correlation of each feature of Buckberry and Chamberlain's method (Table 3) with the curvature variation and found that the increasing expression of the surface texture, in both modalities, and the macroporosity, especially in 3D laser models, were strongly correlated with the curvatures. Indeed, for some variables we found stronger correlations than those reported by Buckberry and Chamberlain in their paper for the Spitalfields sample (10). Changes in surface texture cannot be really detected on 3D models, as reported in previous papers (18, 19) but scores of 4-5 correspond to a progressively irregular surface dominated by the presence of dense bone, consequently with high values of absolute curvature. It may be worth noting that this very feature had been described as "bumps" in the Transitional analysis recording system (20). The same changes occur in auricular surface dominated by macroporosity, especially when present in both demifaces.

During the analysis of the Terry Collection, we considered only the Partial Total Score and we found only moderate correlation in all variables except for the percent of convex surface. The auricular surface is generally more prominent in females and this could explain why the percent of convex did not express variation with increasing age. This trait could possibly be used for sex estimation. The correlations in the auricular surface were stronger than those in the pubic bones, but there is a largely individual dispersion and a large portion of overlapping between scores and decades. Finally, it is interesting to note that in our data the major difference between 3D models from CT and laser acquisition was in the dispersion of the data, not in the general trend. This highlights that the resolution of the 3D models does not play a major role at least in our study; the 3D models from CT scans express in an adequate way the variation of the surface. This was also valid for both the 3D model of the pubic bone and the auricular surface.

Our results do not substantially differ from those of the classical methods; wide estimated age intervals, with width of 58 - 59 years are present for both SB and BC methods (21). The advantage of a quantitative method is the limitation of the subjectivity in its application, since it has been reported that inter-observer agreement varies largely and depends on the method employed (22, 23). However, the process of age estimation is more complicated than just looking at one surface and uncritically matching it with a phase. An automated mathematical system could remove this subjectivity. The best approach is to look at the entire skeleton, have a general impression (young, middle or old adult) and then apply a suitable combination of methods (24). In particular, an expert anthropologist may see signs of illness or other condition which can alter the age-related changes observed. We may say that the final estimation draws largely from experience, as also argued by Garvin and Passalacqua (5).

Many different methodological and statistical approaches have been used to improve the accuracy of age estimation or to combine different existing methods: artificial neural networks (25); nature-inspired data mining methods (26); smoothing procedure (27); transition analysis (20). The new approach we explored utilized the 3D digital nature of CT and laser scans and a single, simple way to mathematically describe the surface changes, namely the extrinsic curvature. We found it encouraging that such a simple procedure, requiring no expert judgment from the operator, achieved moderate correlations with the decades of the actual age at death. It is therefore reasonable to expect that the associated high dispersion of the data would be reduced by the inclusion of further surface properties using the established methods of differential geometry (28). For instance, spatial frequency and directional orientation of the surface features could be calculated, again in a completely automatic way.

Nowadays, many forensic anthropological laboratories have access to a laser scanner, the NextEngine or Minolta being rather widespread (29, 30) , and many departments of Forensic Medicine use CT scanners for routine investigations (31, 32) and these products should be easily accessible by anthropological laboratories. In principle, the performance parameters of each laser scanner and the scanning setting of the CT scanner could influence the results and need to be investigated to evaluate the reproducibility of the quantitative analysis among instruments.

We conclude that further development of our approach has the potential to capture most of the objective surface features routinely observed for age estimation, bypassing the known subjectivity reported by Galera et al. (22), Kimmerle et al. (23) and others. The expert visual assessement by the physical anthropologist could then be focused on the foundamental consideration of the overall condition of the skeleton, taking into consideration pathology for example, which can affect automatic age estimation and that will always require direct specialist evaluation.

Villa C., Buckberry J., Cattaneo C., Frohilich B., Lynnerup N. 2015. *Quantitative analysis of the morphological changes of the pubic symphyseal face and the auricular surface and implications for age at death estimation*. Journal of Forensic Sciences-. Journal of Forensic Sciences, Vol. 60, No. 3, 2015, p. 556–565.

Acknowledgements

We would like to thank the Smithsonian Institution and Dr. David Hunt for allowing us the access to the Terry Collection. We also thank the anonymous reviewers for their constructive comments that helped us to improve the manuscript.

References

1. Todd TW. Age changes in the pubic bone. I. The male white pubis. Am J Phys Anthropol. 1920;3(3):285-334.
2. Acsádi G, Nemeskéri J. History of human life span and mortality. Budapest: Akadémiai Kiadó, 1970.
3. Brooks S, Suchey J. Skeletal age determination based on the Os Pubis: A Comparison of the Acsadi-Nemeskeri and Suchey-Brooks Methods. J Hum Evol. 1990;5:227-38.
4. McKern TW, Stewart TD. Skeletal Age Changes in Young American Males.Technical Report EP-45. Natick, Mass.: Quartermaster Research and Development Command, 1957.
5. Garvin HM, Passalacqua NV. Current practices by forensic anthropologists in adult skeletal age estimation. J Forensic Sci. 2012;57(2):427-33.
6. Suchey JM, Brooks ST, Katz D. Instructions for use of the Suchey-Brooks system for age determination of the female os pubis. Instructional materials accompanying female pubic symphysial models of the Suchey-Brooks system. Fort Collins, Colorado: France Casting. 1988.
7. Sashin D. A critical analysis of the anatomy and the pathological changes of the sacro-iliac joints. Bone Joint Surg. 1930;28:891-910.

Villa C., Buckberry J., Cattaneo C., Frohilich B., Lynnerup N. 2015. *Quantitative analysis of the morphological changes of the pubic symphyseal face and the auricular surface and implications for age at death estimation*. Journal of Forensic Sciences-. Journal of Forensic Sciences, Vol. 60, No. 3, 2015, p. 556–565.

8. Lovejoy CO, Meindl RS, Pryzbeck TR, Mensforth RP. Chronological metamorphosis of the auricular surface of the ilium: a new method for the determination of adult skeletal age at death. Am J Phys Anthropol. 1985;68(1):15-28.
9. Bedford ME, Russell KF, Lovejoy CO. The auricular surface aging technique: 16 color photographs with descriptions. Kent, OH: Kent State University, 1989.
10. Buckberry JL, Chamberlain AT. Age estimation from the auricular surface of the ilium: A revised method. Am J Phys Anthropol. 2002;119(3):231-9.
11. Falys CG, Schutkowski H, Weston DA. Auricular surface aging: worse than expected? A test of the revised method on a documented historic skeletal assemblage. Am J Phys Anthropol. 2006;130(4):508-13.
12. Hens SM, Rastelli E, Belcastro G. Age estimation from the human os coxa: a test on a documented Italian collection. J Forensic Sci. 2008;53(5):1040-3.
13. Biwasaka H, Sato K, Aoki Y, Kato H, Maeno Y, Tanijiri T, et al. Three dimensional surface analyses of pubic symphyseal faces of contemporary Japanese reconstructed with 3D digitized scanner. Leg Med (Tokyo). 2013;15(5):264-8.
14. Da Fontoura Costa L, Jr MCR. Shape Analysis and Classification: Theory and Practice. Boca Raton, Florida: CRC Press LLC, 2000.
15. Peyre G. The Numerical Tours of Signal Processing - Advanced Computational Signal and Image Processing. IEEE Comput Sci Eng. 2011;13(4):94-7.
16. http://www.mathworks.com/matlabcentral/fileexchange/5355 last accessed 20.01.2014

Villa C., Buckberry J., Cattaneo C., Frohilich B., Lynnerup N. 2015. *Quantitative analysis of the morphological changes of the pubic symphyseal face and the auricular surface and implications for age at death estimation*. Journal of Forensic Sciences-. Journal of Forensic Sciences, Vol. 60, No. 3, 2015, p. 556–565.

17. Biwasaka H, Sato K, Aoki Y, Kato H, Maeno Y, Tanijiri T, et al. Three dimensional surface analyses of pubic symphyseal faces of contemporary Japanese reconstructed with 3D digitized scanner. Leg Med (Tokyo). 2013.
18. Telmon N, Gaston A, Chemla P, Blanc A, Joffre F, Rouge D. Application of the Suchey-Brooks method to three-dimensional imaging of the pubic symphysis. J Forensic Sci. 2005;50(3):507-12.
19. Villa C, Buckberry J, Cattaneo C, Lynnerup N. Technical note: Reliability of Suchey-Brooks and Buckberry-Chamberlain methods on 3D visualizations from CT and laser scans. Am J Phys Anthropol. 2013;151(1):158-63.
20. Boldsen JL, Milner GR, Konigsberg LW, Wood JW. Transition analysis: a new method for estimating age from skeletons. In: Hoppa RD, Vaupel JW, editors. Paleodemography : Age Distributions from Skeletal Samples. New York: Cambridge University Press 2002;73-106.
21. San Millan M, Rissech C, Turbon D. A test of Suchey-Brooks (pubic symphysis) and Buckberry-Chamberlain (auricular surface) methods on an identified Spanish sample: paleodemographic implications. J Archaeol Sci. 2013;40(4):1743-51.
22. Galera V, Ubelaker DH, Hayek LC. Interobserver error in macroscopic methods of estimating age at death from the human skeleton. Int J Anthropol. 1995;10(4):229-39.
23. Kimmerle EH, Prince DA, Berg GE. Inter-observer variation in methodologies involving the pubic symphysis, sternal ribs, and teeth. J Forensic Sci. 2008;53(3):594-600.
24. Milner GR, Boldsen JL. Skeletal Age Estimation: Where We Are and Where We Should Go. A Companion to Forensic Anthropology: John Wiley & Sons, Ltd; 2012;224-38.

25. Corsini MM, Schmitt A, Bruzek J. Aging process variability on the human skeleton: artificial network as an appropriate tool for age at death assessment. Forensic Sci Int. 2005;148(2-3):163-7.

26. Buk Z, Kordik P, Bruzek J, Schmitt A, Snorek M. The age at death assessment in a multi-ethnic sample of pelvic bones using nature-inspired data mining methods. Forensic Sci Int. 2012;220(1-3):294 e1-9.

27. Martins R, Oliveira PE, Schmitt A. Estimation of age at death from the pubic symphysis and the auricular surface of the ilium using a smoothing procedure. Forensic Sci Int. 2012;219(1-3):287 e1-7.

28. Banchoff TF, Lovett ST. Differential Geometry of Curves and Surfaces. New York: A K Peters/CRC Press, 2010.

29. Cattaneo C, Cantatore A, Ciaffi R, Gibelli D, Cigada A, De Angelis D, et al. Personal identification by the comparison of facial profiles: testing the reliability of a high-resolution 3D-2D comparison model. J Forensic Sci. 2012;57(1):182-7.

30. Sholts SB, Walker PL, Kuzminsky SC, Miller KW, Warmlander SK. Identification of group affinity from cross-sectional contours of the human midfacial skeleton using digital morphometrics and 3D laser scanning technology. J Forensic Sci. 2011;56(2):333-8.

31. Poulsen K, Simonsen J. Computed tomography as routine in connection with medico-legal autopsies. Forensic Sci Int. 2007;171(2-3):190-7.

32. Thali MJ, Yen K, Schweitzer W, Vock P, Boesch C, Ozdoba C, et al. Virtopsy, a new imaging horizon in forensic pathology: Virtual autopsy by postmortem multislice computed tomography

(MSCT) and magnetic resonance imaging (MRI) - a feasibility study. J Forensic Sci.

2003;48(2):386-403.

Villa C., Buckberry J., Cattaneo C., Frohilich B., Lynnerup N. 2015. *Quantitative analysis of the morphological changes of the pubic symphyseal face and the auricular surface and implications for age at death estimation*. Journal of Forensic Sciences-. Journal of Forensic Sciences, Vol. 60, No. 3, 2015, p. 556–565.

Additional Information and Reprint Requests Section

Chiara Villa, M.Sc.

University of Copenhagen,

Department of Forensic Medicine

Frederik V's Vej 11

DK-2100 Copenhagen

Email**:** chiara.villa@sund.ku.dk

Table 1: Pubic bone casts: Spearman's correlation between phases and the curvature variables in the pubic casts

	CT				**Laser**	
	ROI: anterior area		ROI: central area		ROI: central area	
	F	M	F	M	F	M
Mean	-0.59	-0.04	-0.92***	-0.74**	-0.83***	-0.67*
Highest	-0.43	0.41	-0.93***	-0.76**	-0.89***	-0.67*
Lowest	0.64	0.37	0.83***	0.71**	0.78**	0.62*
Convex	-0.16	-0.38	-0.91***	-0.79**	-0.75***	-0.72*
Flat	0.91	0.75	0.93***	0.6*	0.91**	0.75*

*** p<0.001** p<0.01 *p<0.05

Table 2 Pubic bones from the Terry Collection: Spearman's correlation between phases / decades and the curvature variables

		CT		**Laser**	
		F	M	F	M
Mean	vs SB phases	0.29*	0.06	0.29*	0.20
	vs Decades	0.17	-0.04	0.27	0.03
Highest	vs SB phases	0.12	0.27	0.31*	0.09
	vs Decades	0.20	0.22	0.21	-0.05
Lowest	vs SB phases	0.22	-0.37*	-0.27	-0.26
	vs Decades	0.29	-0.21	-0.32*	-0.03
Convex	vs SB phases	0.003	-0.27	-0.05	-0.29
	vs Decades	-0.09	-0.32*	-0.10	-0.51*
Flat	vs SB phases	-0.33*	0.09	-0.29*	-0.21
	vs Decades	0.14	0.04	-0.30*	-0.02

*p<0.05

Table 3: BC “recording kit”: Spearman’s correlation between the curvature variables and Partial Total Score / Transverse Organization/Surface Texture/Macroporosity / Microporosity

	CT					**Laser**				
	Partial Total score	TO	ST	MA	MI	Partial Total score	TO	ST	MA	MI
Mean	0.56*	0.38	0.68***	0.52*	0.20	0.40	0.06	0.52*	0.64**	0.15
Highest	-0.30	-0.48*	-0.27	0.06	-0.12	0.44	-0.03	0.55*	0.75***	0.15
Lowest	-0.43	0.39	0.65**	-0.23	0.04	-0.48*	-0.16	-0.61**	-0.64**	-0.13
Convex	-0.37	-0.50*	0.38	0.01	-0.02	0.09	-0.33	-0.13	0.21	0.33
Flat	-0.53*	-0.47*	0.60**	-0.41	0.11	-0.41*	-0.05	-0.50*	-0.64**	-0.21

*** p<0.001;** p<0.01; *p<0.05 (TO = transverse organization; ST = surface texture, MA= macroporosity, MI= microporosity)

Table 4: Auricular surfaces from the Terry Collection: Spearman’s correlation between Partial Total Score / decades and the curvature variables

		CT	**Laser**
Mean	Partial Total Score	0.41**	0.45**
	Decades	0.42**	0.40**
Highest	Partial Total Score	0.33**	0.49**
	Decades	0.34**	0.42**
Lowest	Partial Total Score	-0.43**	0.44**
	Decades	-0.46**	0.42**
Flat	Partial Total Score	-0.33**	0.50**
	Decades	-0.32**	0.44**
Convex	Partial Total Score	-0.17	0.19
	Decades	0.002	0.06

** p<0.01

Table 5: The descriptive statistics of four of the curvature variables (mean, highest, lowest, flat) versus the decades for CT and Laser modalities

			CT					Laser				
Mean (*100)	**Decades**	**N**	**Mean**	**SD**	**Min**	**Max**	**Median**	**Mean**	**SD**	**Min**	**Max**	**Median**
	<39	9	0.858	0.383	0.572	1.837	0.756	0.44	0.067	0.364	0.581	0.433
	40-49	16	0.839	0.22	0.554	1.396	0.789	0.433	0.075	0.34	0.605	0.418
	50-59	22	0.945	0.315	0.569	1.779	0.848	0.449	0.061	0.367	0.597	0.434
	60-69	20	0.975	0.179	0.712	1.288	0.929	0.5	0.086	0.41	0.688	0.471
	70-79	17	1.116	0.531	0.533	2.354	0.873	0.528	0.123	0.369	0.774	0.507
	80-89	14	1.59	0.829	0.848	3.705	1.30	0.558	0.142	0.391	0.834	0.533
Highest (*100)	**Decades**	**N**	**Mean**	**SD**	**Min**	**Max**	**Median**	**Mean**	**SD**	**Min**	**Max**	**Median**
	<39	9	1.62	0.472	1.085	2.644	1.414	0.965	0.143	0.812	1.219	0.904
	40-49	16	1.572	0.336	0.882	2.002	1.603	0.951	0.187	0.741	1.366	0.921
	50-59	22	1.93	0.509	1.219	3.076	1.961	1.027	0.134	0.785	1.329	1.03
	60-69	20	1.999	0.388	1.27	2.618	2.044	1.123	0.187	0.862	1.428	1.111
	70-79	17	1.799	0.685	0.609	2.963	1.602	1.17	0.277	0.77	1.633	1.102
	80-89	14	2.443	0.712	1.673	4.116	2.158	1.28	0.336	0.926	1.957	1.225
Lowest (*100)	**Decades**	**N**	**Mean**	**SD**	**Min**	**Max**	**Median**	**Mean**	**SD**	**Min**	**Max**	**Median**
	<39	9	-2.48	1.886	-7.445	-1.325	-1.816	-1.11	0.207	-1.49	-0.85	-1.137
	40-49	16	-2.448	1.079	-5.521	-0.987	-2.154	-1.052	0.176	-1.37	-0.74	-1.052
	50-59	22	-2.535	1.279	-5.832	-1.209	-2.226	-1.078	0.196	-1.57	-0.828	-1.054
	60-69	20	-2.79	1.12	-4.902	-1.20	-2.839	-1.222	0.237	-1.80	-0.87	-1.161
	70-79	17	-3.492	1.777	-6.89	-1.49	-2.996	-1.354	0.352	-2.07	-0.90	-1.275
	80-89	14	-4.98	2.224	-9.636	-1.854	-4.588	-1.415	0.357	-2.18	-0.99	-1.361
Flat	**Decades**	**N**	**Mean**	**SD**	**Min**	**Max**	**Median**	**Mean**	**SD**	**Min**	**Max**	**Median**
	<39	9	65.521	11.692	38.289	74.918	69.341	95.857	2.736	90.58	99.02	95.931
	40-49	16	68.414	9.832	53.257	86.717	65.84	96.256	2.993	88.72	99.61	97.184
	50-59	22	63.778	10.655	35.667	79.024	64.322	95.824	2.471	88.37	98.75	96.454
	60-69	20	61.238	8.662	47.322	81.326	61.74	93.709	3.565	86.26	97.44	95.14
	70-79	17	61.239	15.239	38.877	89.786	63.391	92.23	5.513	80.71	97.66	94.036

	80-89	14	51.838	14.003	22.598	70.081	53.281	90.625	6.26	77.51	96.68	92.408

Fig. 1 - Sex and age distribution of the Terry Collection sample

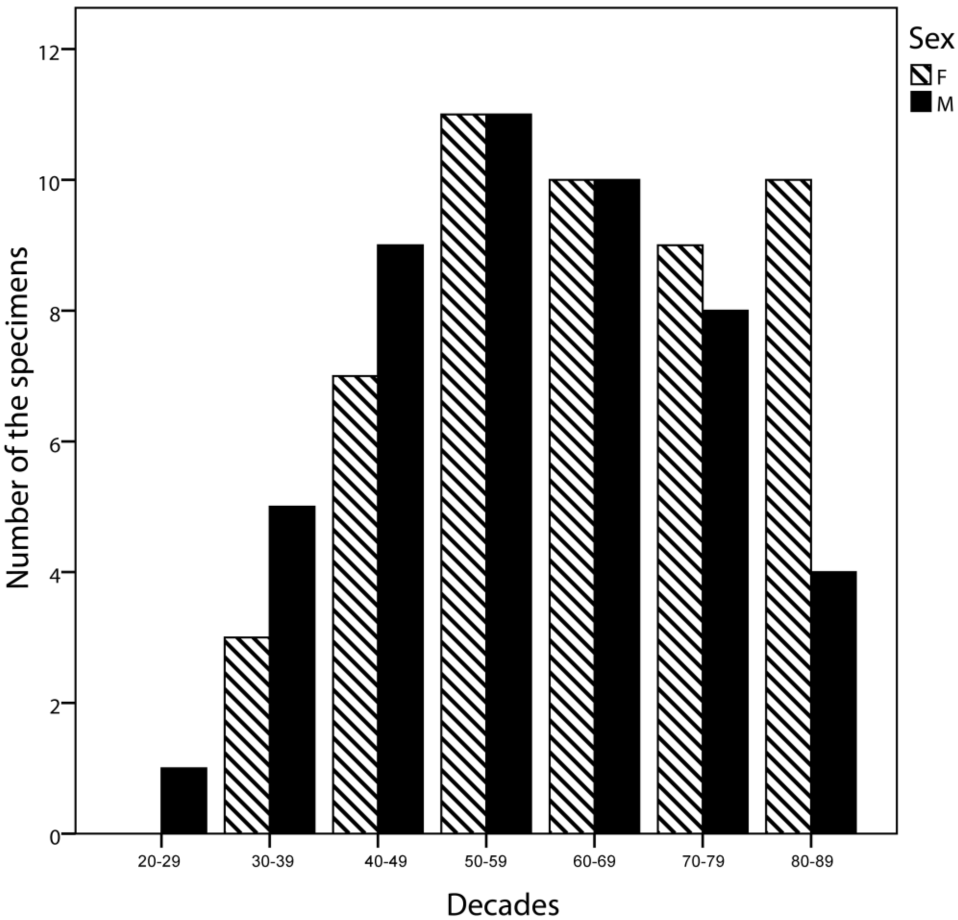

Fig. 2 - Regions of interest (ROIs): a, anterior portion of the pubic bone; b, central portion of the pubic symphyseal face; c, internal portion of the auricular surface.

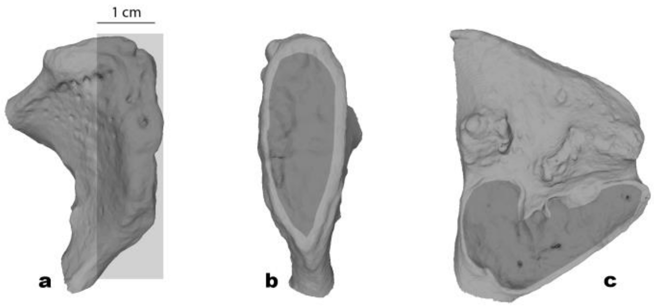

Fig. 3 - Color coded images of the results of the curvature analysis on the 12 female SB pubic bone casts: blue represents concave areas in the bar (i.e. furrows); red represents convex areas (i.e ridges); green represents the flat surfaces.

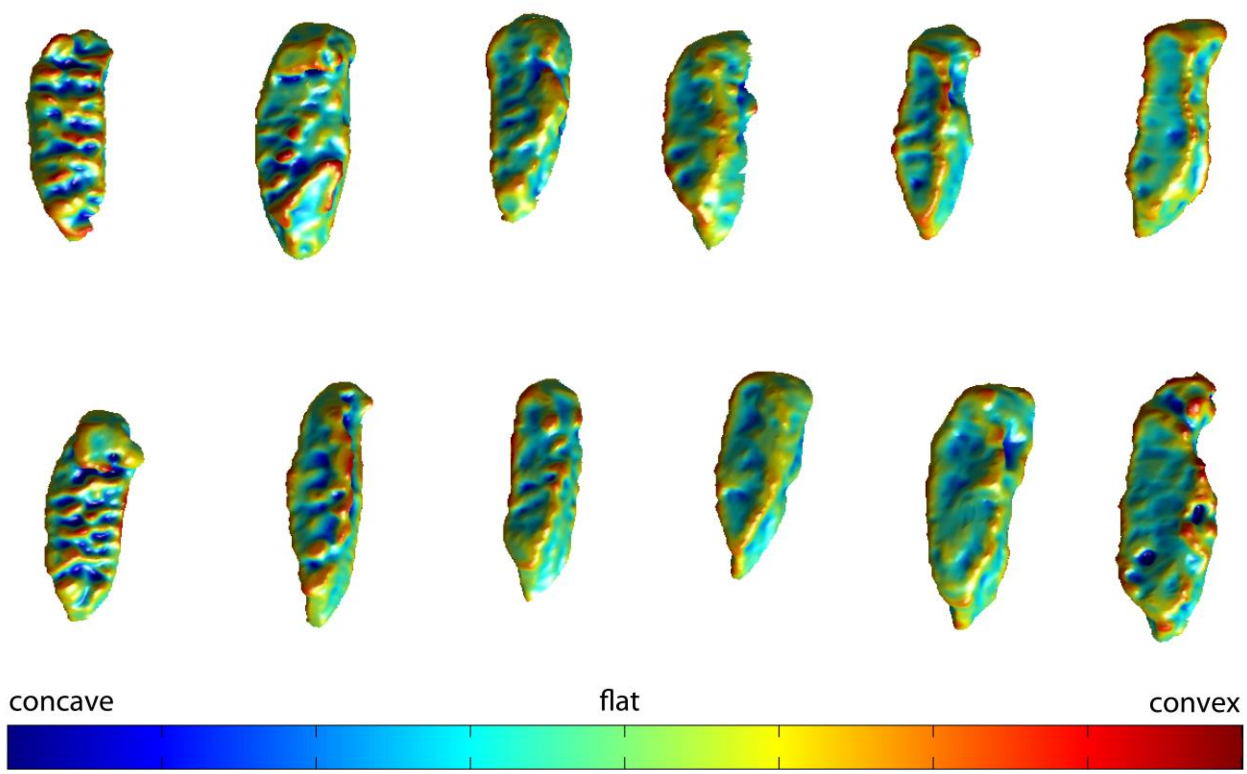

Fig. 4 - Pubic bones, SB casts: scatter plots of the arithmetic mean of the absolute values of curvature (mean, left column) and the percent of the flat surface (flat, right column) versus the phases marked by sex. In the top row the results for 3D models from the CT scans, in the bottom row for the 3D models from laser scanner.

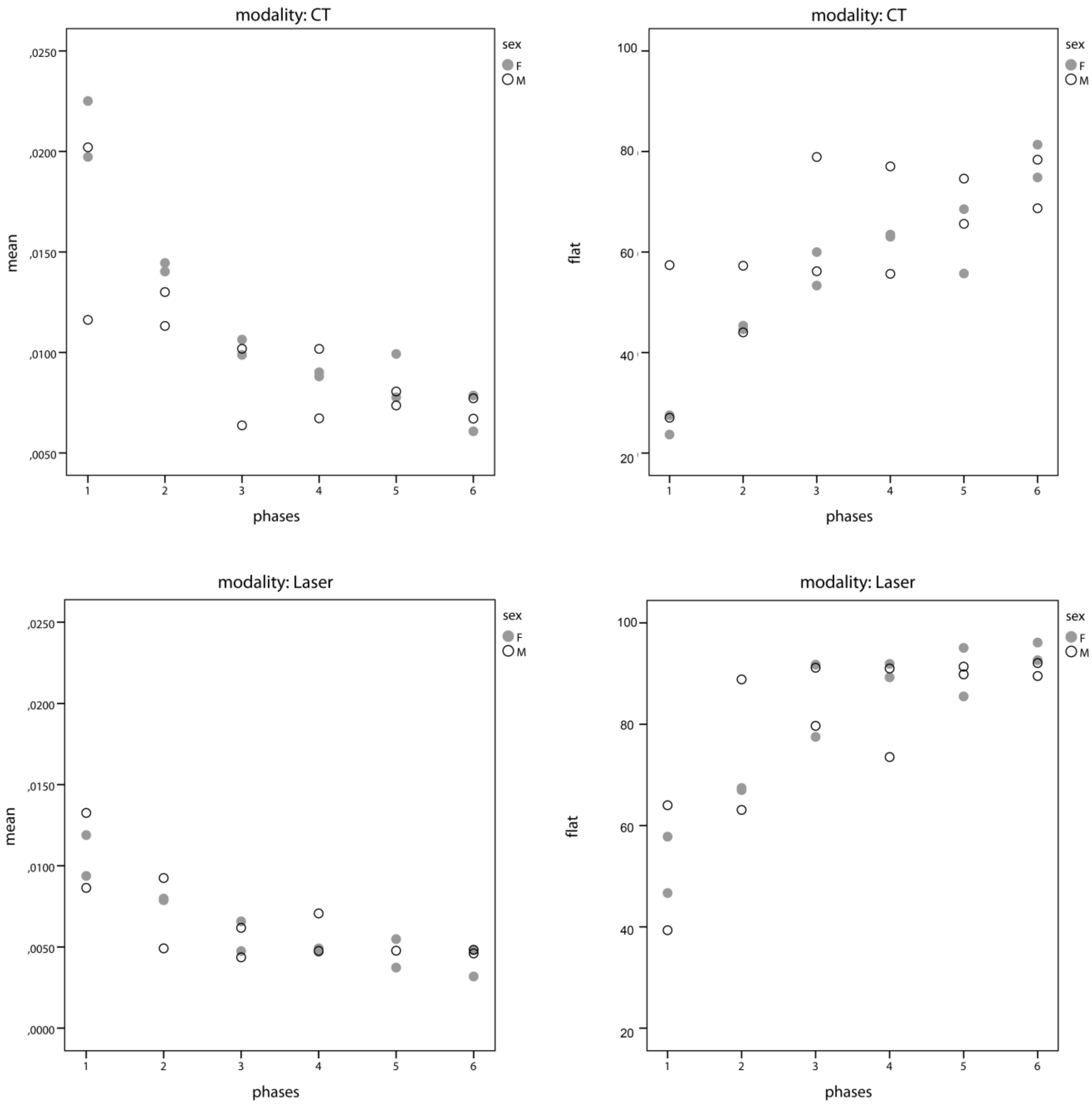

Fig. 5 - Pubic bones, Terry Collection: scatter plots of the arithmetic mean of the absolute values of curvature (mean, left column) and the percent of convex surface (convex, right column) versus the phases (left column) and the decades (right column). In the top row the results for 3D models from the CT scans, in the bottom row for the 3D models from laser scanner.

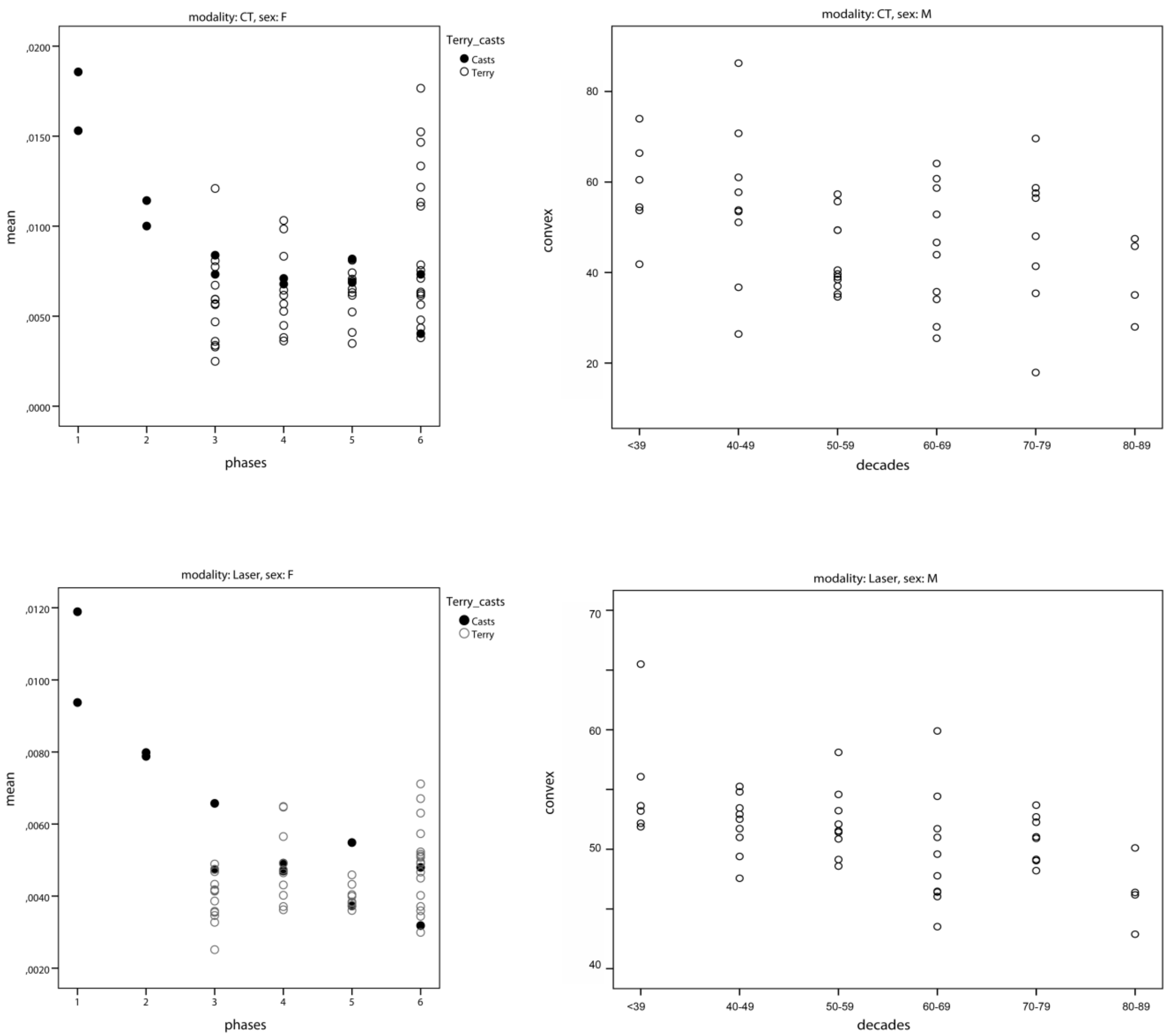

Fig. 6 - Auricular surfaces, BC ”recording kit”: scatter plots of the arithmetic mean of the absolute values of curvature (mean, left column) and the percent of the flat surface (flat, right column) versus the Partial total score marked by modality.

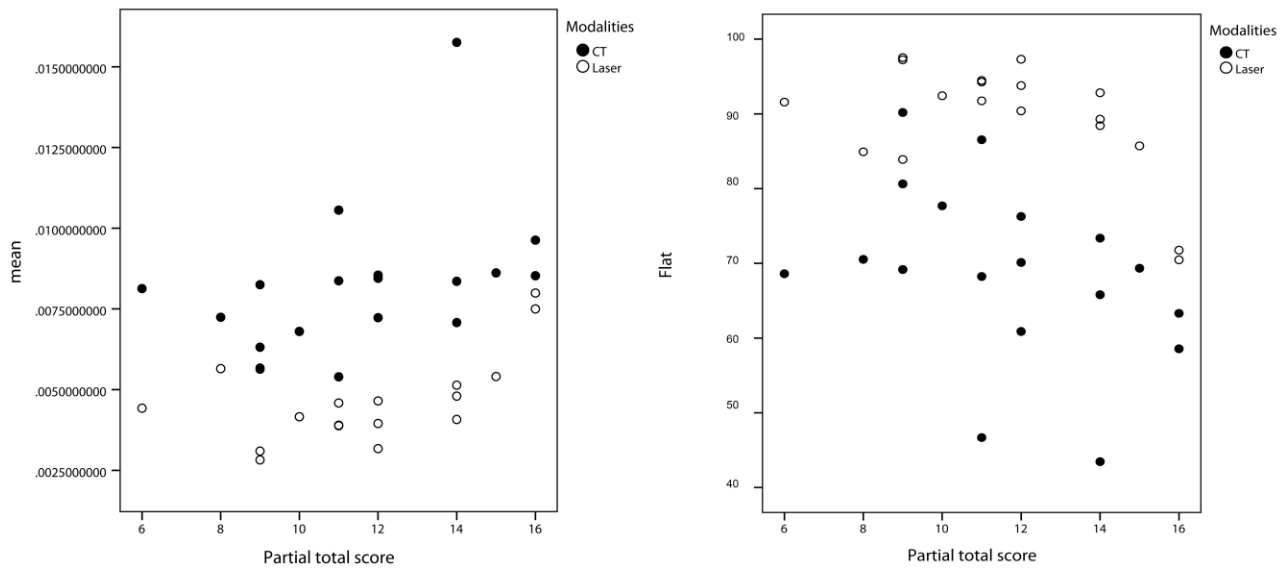

Villa C., Buckberry J., Cattaneo C., Frohilich B., Lynnerup N. 2015. *Quantitative analysis of the morphological changes of the pubic symphyseal face and the auricular surface and implications for age at death estimation*. Journal of Forensic Sciences-. Journal of Forensic Sciences, Vol. 60, No. 3, 2015, p. 556–565.

Fig. 7 - Auricular surfaces, Terry Collection: scatter plots of the lowest ten percent of the the curvature values (lowest, top row) and the percent of the flat surface (flat, bottom row) versus the Partial total score (left column) and the decades (right column).